

Final Outcomes Report

CCEMC Project ID: K130098

**Chemical Transformation of Carbon Dioxide via Solar-Powered
Artificial Photosynthesis**

Prof. Zetian Mi

**Department of Electrical and Computer Engineering
McGill University
3480 University Street
Montreal, QC H3A 0C6
Canada**

E-mail: zetian.mi@mcgill.ca; Phone: 1 514 398 7114

Project Advisor: Dr. Surindar Singh

Completion date of the project: March 31, 2016

CCEMC and Her Majesty the Queen in right of Alberta and each of them make no warranty, express or implied, nor assume any legal liability or responsibility for the accuracy, completeness, or usefulness of any information contained in this publication, nor that use thereof does not infringe on privately owned rights. The views and opinions of the author expressed herein do not necessarily reflect those of CCEMC and Her Majesty the Queen in right of Alberta and each of them. The directors, officers, employees, agents and consultants of CCEMC and the Government of Alberta are exempted, excluded and absolved from all liability for damage or injury, howsoever caused, to any person in connection with or arising out of the use by that person for any purpose of this publication or its contents.

Submitted on May 29, 2016

1. Introduction – Brief description of the project

Nowadays, the world energy use is primarily based on fossil fuels (i.e. coal, petroleum, and natural gas). The heavy reliance on fossil fuels for the production of energy results in emissions of 30.4 Gt of carbon dioxide (CO₂) into the atmosphere.¹ CO₂ is one of the major greenhouse gases and at present CO₂ emission in the world is increasing at a high rate.² One option for reducing CO₂ emissions is to capture a portion of the CO₂ from large point sources that would otherwise be emitted and store it in a location that isolates it from the atmosphere on time scales of centuries to millennia. Geographical formations, such as declining oil fields, unmineable coal seams, and deep oceans have been proposed and utilized to sequester CO₂. However, the long-term effectiveness and safety of these approaches, as well as any associated environmental impact, including ocean acidification has remained unclear. Alternatively, CO₂ can be chemically transformed into hydrocarbons, which can be readily stored in the form of liquid or solid. More importantly, such value-added products have wide marketability and can significantly reduce, or even offset the cost associated with CO₂ capture.³⁻⁸

Since the chemical transformation of CO₂ into hydrocarbons is an endothermic process, conventional approaches generally involves the use of very high temperature, high pressure, and/or extremely reactive reagents.³ As a consequence, this process is neither economically feasible nor environmentally friendly. In this project, we proposed to develop a CO₂ transformation system with the use of sunlight as the energy input. The solar-powered technology, by mimicking the natural photosynthesis process, converts CO₂ and non-potable water into commercially-valuable chemical products, including methane (CH₄), hydrogen (H₂), oxygen (O₂), and methanol (CH₃OH). These value-added products have wide marketability and can offset the cost associated with CO₂ capture. In the process, the solar energy is directly converted into storable chemical fuels and, at the same time, greenhouse gas emission is mitigated from the atmosphere.⁹⁻¹⁵

To date, a number of ongoing projects are developing this technology around the world. In this project, we have developed an efficient photocatalyst, with the use of metal-nitride nanowires, which can help overcome the efficiency bottleneck of conventional photocatalytic technologies.¹⁶⁻¹⁸ The photocatalyst is extremely stable and no efficiency degradation is measured during long-term operation. The photocatalytic route involves only the use of CO₂, sunlight and water, and the CO₂ hydrogenation reaction takes place at room temperature. More importantly, this technology can be performed directly on site to utilize CO₂ emissions and wastewater generated during oil refinery.

The materials being used for this technology development are well established in the semiconductor industry. Today, large quantities of metal-nitride semiconductor wafers have been widely produced in the solid-state lighting and power electronics industries.¹⁹ The rapid development of these industries has led to drastically reduced cost for the mass production of these materials. Therefore our technology is entirely scalable and cost effective. This project aims to demonstrate CO₂ reduction to hydrocarbon fuels, which was successfully achieved during the course of this project.

Our CO₂ chemical transformation system represents a completely new approach and will result in a novel product slate that can be tailored for each end-user. Producers can harness CO₂ and recycle non-potable water into commercially valuable chemicals such as methane, hydrogen, oxygen or methanol. For the end-user, it is not a comparison between the cost of the system (operating and capital) versus the cost of emitting CO₂ but rather an opportunity to manage CO₂ emissions as either a cost-neutral or possible revenue-generating operation. The technology is an excellent fit for the oil sands as all the materials can either generated or used on-site, with no additional requirements.

2. Project outcomes

In this two-year project, we have demonstrated a proof-of-concept modular system that can selectively convert carbon dioxide into various hydrocarbon fuels, including methane and methanol. This technological breakthrough was made possible by our innovations in metal-nitride nanowire photocatalysts.

2.1 Synthesis of Metal-Nitride Semiconductor Photocatalysts

Gallium nitride based quantum well devices, including LEDs and power transistors have been widely commercialized today. And the use of gallium nitride nanowire technology can break the fundamental efficiency bottleneck of solar fuels generation. However, the growth and synthesis of such nanowire devices is different from the conventional quantum well structures. To realize high efficiency nanowire-based devices, it requires the unique ability to grow defect-free GaN nanowires. In the past several years, we have pioneered in the development of large area nanowire growth and their applications in solar fuels production. It is worthwhile mentioning that very recently there are already a few companies working on the commercialization of GaN-based nanowire devices. Two key technology developments are listed below.

We have invented the catalyst-free epitaxy of InN nanowires, now widely used for the growth/synthesis of III-nitride nanowire arrays. In this growth process, an in situ deposited indium or gallium layer serves as the seeding layer, which can promote the formation and nucleation of InGa_xN nanowire arrays. With the use of technique, superior quality metal-nitride nanowire arrays can be formed directly on Si substrate, which enables the integration of nanowire photocatalysts with low cost, large area Si solar cell wafers, thereby leading to scalable production of solar fuels.

We have invented high efficiency broadband semiconductor nanowire devices. We have invented the process for achieving self-organized, broadband quantum-confined nanostructures that can harvest most of the solar spectrum. Such quantum-confined nanostructures are free of defects and dislocations, and the alloy compositions can be tuned over a broad range by simply changing the flux ration during the synthesis/growth process.

2.2 Characterization of Nanowire Photocatalysts

We have performed detailed structural and optical characterization of the metal-nitride nanowires using scanning electron microscopy (SEM) and transmission electron microscopy

(TEM), and photoluminescence (PL) studies. Fig. 1a illustrates InGaN/GaN multiple-quantum-dot nanowire LED heterostructure grown by PAMBE under N-rich conditions. Detailed structural and elemental characterizations were performed using scanning transmission electron microscopy (STEM). Fig. 1b shows high resolution TEM image of multiple-active-region (MAR) tunnel junction (TJ) dot-in-a-wire LED structure. No phase segregation or dislocations were observed in InGaN nanowires, demonstrating excellent crystalline quality of the nanowires. High angle annular dark field (HAADF) image (Fig. 1c) further showed the MAR TJ dot-in-a-wire LED structure with the presence of tunnel junctions and quantum dot active regions. EDXS line profile along c-axis (growth direction) revealed In peaks in the tunnel junctions and Ga dips and In peaks in dot region (lower panel in Fig. 1c). In order to enhance the photocatalytic activity of the as-grown nanowires, Rh/Cr₂O₃ nanoparticles were photodeposited onto the nanowires, as illustrated in the electron energy loss spectroscopy (EELS) image in Fig. 1e. The Rh (core) nanoparticles enhance the charge carrier extraction and the Cr₂O₃ (shell) suppress the back reaction of water formation from the evolved H₂ and O₂.

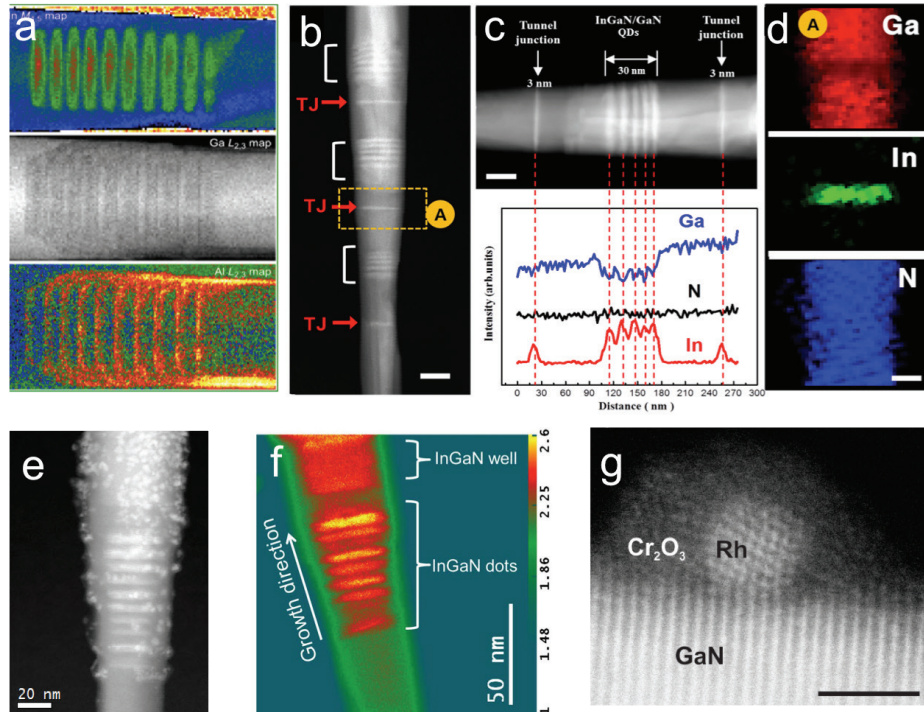


Fig. 1. (a) Elemental mapping result showing distributions of In, Ga, and Al elements within the nanowire LED structure. (b) HRTEM of multiple-active-region (MAR) tunnel junction (TJ) dot-in-a-wire LED structure. (c) High angle annular dark field (HAADF) image showing the MAR TJ dot-in-a-wire LED structure with the presence of tunnel junctions and quantum dot active regions. EDXS line profile along c-axis (growth direction) showing In peaks in the tunnel junctions and Ga dips and In peaks in dot region (lower panel). (d) EDXS elemental mapping image of tunnel junction region showing the In, Ga, and N variations. (e) Electron energy loss spectroscopy (EELS) image of Rh/Cr₂O₃ core/shell nanoparticles decorated triple-band InGaN/GaN nanowire. (f) High angle annular dark field (HAADF) image in pseudocolor display of an as-grown InGaN/GaN nanowire heterostructure, showing the atomic number contrast between InGaN (red) and GaN (green) layers. (g) STEM-HAADF image of Rh/Cr₂O₃ (core/shell) nanoparticle-decorated GaN:Mg nanowire.

2.3 Solar Water Splitting and Hydrogen Generation

We have invented a powerful surface engineering technique that can significantly enhance the efficiency of solar-to-hydrogen conversion. We have demonstrated that with controlled amount of *p*-type Mg dopant incorporation during the epitaxial growth process in *N*-rich condition, the near-surface band bending on the nonpolar surface (*m*-planes) of GaN nanowire can be precisely tuned. By tuning the band bending on the nonpolar surfaces of GaN nanowires using *p*-type Mg doping, an absorbed photon conversion efficiency (APCE) of $\sim 51\%$ was achieved under UV light, which was nearly two orders of magnitude higher than undoped GaN, shown in Fig. 2. Repeated cycles of overall water splitting further confirmed a high level of stability of the Mg doped GaN nanowire photocatalyst.

The performance of the multi-bandgap photosystem is significantly higher than the single-bandgap system due to better matching and utilization of the incident solar spectrum. A multi-band photosystem allows suppressing energy loss due to thermal relaxation of high-energy electrons (except the hot carriers). Consequently, the InGaN/GaN nanowire heterostructure was designed to form a multi-band nanowire photocatalyst. We demonstrated that by optimizing the near-surface band bending, the photocatalytic activity of InGaN nanowires can be enhanced by nearly 30 times compared to undoped samples. An APCE of $\sim 69\%$ was demonstrated under part of the visible light.

We have demonstrated Si-based double band photocathode. In a PEC system, to harvest a wider wavelength range of sunlight, a relatively narrow bandgap photoelectrode is often used, which, however, requires an external bias to produce hydrogen, due to its insufficient photovoltage. One of the solutions to overcome the bottleneck of the low photovoltage of single-photoelectrodes is to implement a buried junction below the photocatalyst (known as photovoltaic-PEC or PV-PEC). We have developed a Si/GaN/*p*-InGaN PV-PEC device heterostructures which consists of a planar n^+ -*p* Si solar cell wafer, ~ 150 nm *n*-GaN and ~ 600 nm *p*-InGaN nanowire segments along the axial direction (Fig. 3a). The top *p*-InGaN nanowire arrays are designed to absorb the ultraviolet and a large portion of the visible solar spectrum. The remaining photons with wavelengths up to $1.1 \mu\text{m}$ are absorbed by the underlying planar Si *p*-*n* junction. In contrary to conventional semiconductor photocatalysts, InGaN can uniquely straddle water oxidation and hydrogen reduction potentials under deep visible light irradiation. The *n*-GaN and *p*-InGaN are connected via an n^+ -GaN/InGaN/ p^{++} -GaN polarization-enhanced tunnel junction, which enables the transport of photo-excited holes from the *p*-InGaN to the *n*-GaN within each single nanowire. This device differs from conventional PV-PEC electrodes in that both the top *p*-InGaN and the bottom GaN/Si light absorbers can simultaneously drive proton reduction due to the lateral photocathode, which can surpass the current matching requirements of conventional tandem electrode. A maximum power conversion efficiency of 8.7% was achieved at 0.33 V vs. NHE. A

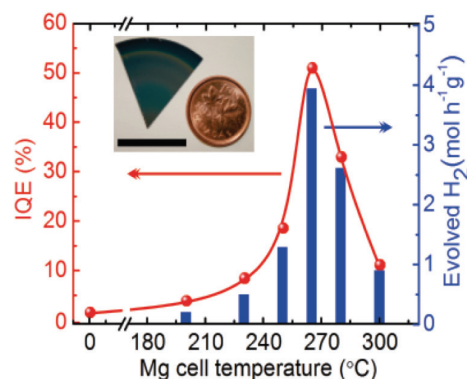


Fig. 2. H₂ evolution rate and internal quantum efficiency (IQE) for different GaN:Mg samples in overall neutral water splitting.

large fraction of the injected electrons can drive proton reduction on GaN surfaces, with the rest carrier extraction scheme of nanowires. That is, due to the relatively small offset between the n^+ -

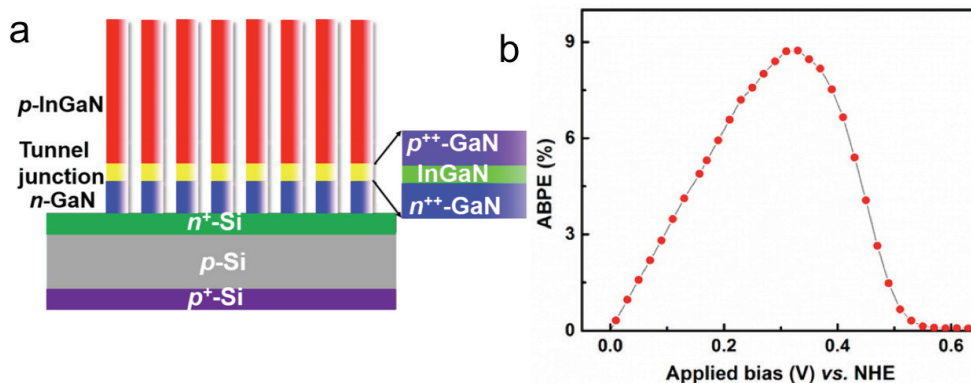


Fig. 3. (a) Schematic of the photocathode grown on n^+ - p Si solar cell substrate. The n -GaN and p -InGaN nanowire segments are connected by an n^{++} -GaN/InGaN/ p^{++} -GaN polarization-enhanced tunnel junction, as shown in the inset. (b) Applied-bias-to-photon-conversion-efficiency (ABPE) vs. applied bias (vs. NHE) of the photocathode in 1M HBr electrolyte under 1.3 sun illumination.

Si and n -GaN conduction band edges, photo-excited electrons of the bottom Si solar cell can readily inject into the n -GaN nanowire segment. It is seen that such a novel design, with the use of Si/GaN-nanowire as the bottom light absorber, can surpass the restriction of current matching in conventional dual absorber devices and simultaneously provide energetic photo-excited electrons to the hydrogen-evolution-reaction (HER) catalyst. Compared to the conventional PEC-PV, such adaptive junction can reduce chemical loss by allowing charge carriers with different overpotentials to be utilized for HER. The Faradaic efficiency for hydrogen generation was also measured to be nearly 100%.

2.4 CO₂ Photoreduction

We have Demonstrated CO₂ reduction into methane and methanol using InGaN nanowires under sunlight illumination. We have demonstrated that CO₂ can be spontaneously activated on the clean surfaces of wurtzite Ga(In)N. We have further demonstrated, for the first time, the photoreduction of CO₂ into methanol can be achieved using sunlight as the only energy input on InGaN nanowire arrays.

Moreover, we have invented a metal-nitride nanowire/Si solar cell photocathode for the reduction of CO₂ to methane under simulated sunlight illumination. Schematically shown in Fig. 4a, the photocathode consists of a planar n^+ - p Si solar cell wafer and n -GaN nanowire arrays. The Si solar cell functions as both the substrate and the photon absorber. Unique to such a monolithically integrated photocathode is that the Si solar cell substrate can harvest a large part of the solar spectrum and the GaN nanowires can significantly enhance the extraction of photo-generated electrons. With the incorporation of Cu co-catalyst on GaN nanowire arrays, we have measured the direct conversion of CO₂ into CH₄ and CO, as shown in Fig. 4b. The Faradaic efficiency can reach ~19 % for the $8e^-$ photoreduction to CH₄, which is more than 30 times higher than that for the CO (~0.6%). Detailed studies further suggest the synergistic effect of GaN nanowires and Cu co-catalyst in significantly enhancing the selectivity for the

photoreduction of CO₂ to CH₄. The GaN nanowire/Si solar cell photocathode also showed excellent stability towards CO₂ reduction.

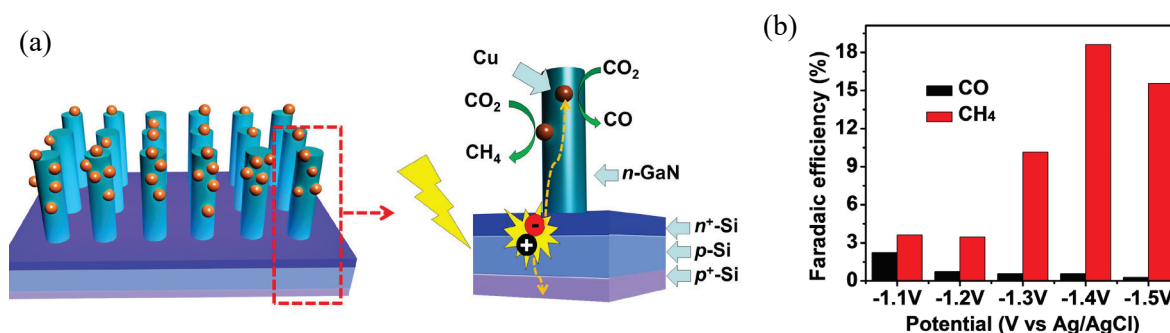


Fig. 4. (a) Schematic illustration of the Cu/GaN/n⁺-p Si photocathode. (b) The measured Faradaic efficiency of Cu/GaN/n⁺-p Si photocathode for different reaction products at different potentials from -1.1 V to -1.5 V (vs Ag/AgCl) in CO₂-saturated aqueous solution of 0.5 M KHCO₃ (pH 8).

3. Conclusions

In summary, we have developed a new CO₂ transformation system powered by sunlight and/or electricity. The technology includes metal-nitride nanowire arrays and their direct integration with low cost, large area Si wafers. We have further experimentally demonstrated that such system can lead to relatively efficient solar fuels generation through photoreduction of carbon dioxide and water splitting. The stability, scalability, and performance of such solar fuels production have also been thoroughly analyzed. We have also engaged with an entrepreneur and are currently in the stage of commercialization. In Round II, we will further improve the efficiency and reduce the cost, and develop a field deployable unit to further evaluate the performance and lifecycle analysis.

References:

1. S. N. Habisreutinger, L. Schmidt-Mende and J. K. Stolarczyk, *Angew Chem Int Ed* **52**, 7372-7408 (2013).
2. Earth's CO₂ Home Page, <https://www.co2.earth/>
3. S. Toshiyasu, J.-C. Choi and H. Yasuda, *Chem Rev* **107**, 2365 (2007).
4. A. O. George, *Angew Chem Int Ed* **44**, 2636 (2005).
5. M. Halmann, *Nature* **275**, 115-116 (1978).
6. B. Aurianblajeni, M. Halmann and J. Manassen, *Solar Energy* **25**, 165-170 (1980).
7. M. Anpo and K. Chiba, *J Mol Catal* **74**, 207-212 (1992).
8. O. K. Varghese, M. Paulose, T. J. LaTempa and C. A. Grimes, *Nano Lett* **9**, 731-737 (2009).
9. T. Inoue, A. Fujishima, S. Konishi and K. Honda, *Nature* **277** (5698), 637-638 (1979).
10. N. Serpone, E. Borgarello and M. Gratzel, *J Chem Soc Chem Comm* (6), 342-344 (1984).
11. O. K. Varghese, M. Paulose, T. J. LaTempa and C. A. Grimes, *Nano Lett* **9** (2), 731-737 (2009).
12. S. N. Habisreutinger, L. Schmidt-Mende and J. K. Stolarczyk, *Angew Chem Int Ed* **52** (29), 7372-7408 (2013).
13. Y. Izumi, *Coordin Chem Rev* **257** (1), 171-186 (2013).
14. S. C. Roy, O. K. Varghese, M. Paulose and C. A. Grimes, *Acs Nano* **4** (3), 1259-1278 (2010).
15. S. Fujita, M. Usui, H. Ito and N. Takezawa, *J Catal* **157** (2), 403-413 (1995).
16. M. G. Kibria, H. P. T. Nguyen, K. Cui, S. Zhao, D. Liu, H. Guo, M. L. Trudeau, S. Paradis, A.-R. Hakima and Z. Mi, *Acs Nano* **7** (9), 7886-7893 (2013).

17. B. AlOtaibi, H. P. T. Nguyen, S. Zhao, M. G. Kibria, S. Fan and Z. Mi, *Nano Lett* **13** (9), 4356-4361 (2013).
18. D. F. Wang, A. Pierre, M. G. Kibria, K. Cui, X. G. Han, K. H. Bevan, H. Guo, S. Paradis, A. R. Hakima and Z. T. Mi, *Nano Lett* **11** (6), 2353-2357 (2011).
19. Y. Nanishi, *Nat Photonics* **8**, 884–886 (2014).